Supplemental Material
Spectroscopy along Flerovium Decay Chains: Discovery of ^{280}Ds and an Excited State in ^{282}Cn

The Supplemental Material provides detailed results and statistical assessments in the analysis of events stemming from decay chains starting with isotopes ^{286,288}Fl. Table I summarizes the information on correlated α-decay chains, which were observed in the present experiment, and which were associated with decays of the even-even isotopes ^{286,288}Fl.

Decay properties such as decay energies and lifetimes, relating to various ensembles of data associated with previous experiments in the direct or indirect production of ^{286,288}Fl and with the present experiment (cf. Table I), are compiled: Distributions of decay energies and correlation times along with determined E_α and $T_{1/2}$ values are presented for the different ensembles in Figs. 1 and 2 for ^{286}Fl and ^{288}Fl, respectively. An overview, together with a statistical assessment of the correlation times attributed to the single decay steps relevant to the current study, is presented Table II for the ensembles of decay chains corresponding to Figs. 1 and 2.

TABLE I: Information on observed correlated α-decay chains suggested to stem from the even-even flerovium isotopes ^{286}Fl and ^{288}Fl. Mid-target beam energies in the laboratory frame, $\langle E_{\rm lab}\rangle$, and the center-of-mass frame, $\langle E_{\rm com}\rangle$, as well as target isotope are provided. Energies of the implanted recoils, $E_{\rm rec}$, the implantation detector strip numbers in x and y, and the assigned isotope of chain origin are listed for each chain. For each decay step, i, the decay energy, E_i, correlation time, Δt_i, and, if in prompt coincidence, photon energies, $E_{\rm ph}$, and electron energies, E_{e-}, are given. In case of a spontaneous fission (SF) event, the number of prompt hits in the Ge-detector crystals, $N_{\rm Ge}$, is provided instead of any specific photon energy. $N_{\rm random}$ indicates the number of chains of a given type expected to arise from random background. Entries in bold were recorded during beam-off periods. Entries in italics relate to tentative or insecure assignments, typically in connection with a missing event in a chain. Uncertainties of individual energy measurements are ≤ 10 keV at typical α-decay energies of 9-10 MeV in the implantation detector. This uncertainty is worse, ≈ 20 keV, for reconstructed events because of the energy straggling in the deadlayers of the Si detectors. See Ref. [20] for more details.

No.	$\langle E_{\rm lab}\rangle$ (MeV) $\langle E_{\rm com}\rangle$ (MeV) target[a]	$E_{\rm rec}$ (MeV) pixel (x,y) isotope	E_1 (MeV) Δt_1 (s) E_{ph} (keV) $E_{e\text{-}}$ (MeV)	E_2 (MeV) Δt_2 (s) E_{ph} (keV) $E_{e\text{-}}$ (MeV)	E_{SF} (MeV) Δt_{SF} (s) $N_{\rm Ge}$	$N_{\rm random}$
01	241 37.8 ^{242}Pu[a]	13.7 (1,14) ^{286}Fl	**10.16(1)**[b] **0.202** [c] -		**250** **0.00161** **3**	$8 \cdot 10^{-7}$
02	241 37.8 ^{242}Pu[a]	13.6 (13,3) ^{286}Fl	**9.60(1)**[b] **0.0526** [d] **0.36(1)**[e]		**239** **0.00148** **11**	$8 \cdot 10^{-7}$
03	238;237 35.1;36.5 $^{242;244}$Pu[a]	14.9 (1,17) $^{286;288}$Fl	**5.68(1)**[f] **0.101** [c] -		**210** **0.0264** **5**	$7 \cdot 10^{-3}$
04	237 36.5 ^{244}Pu	11.3 (18,12) ^{288}Fl	**9.91(1)**[g] **0.0491** [d] -		**246** **0.142** **5**	$8 \cdot 10^{-7}$
05	237 36.5 ^{244}Pu	14.7 (16,14) ^{288}Fl	9.91(1) 4.657 - -		224 0.101	0.02
06	237 36.5 ^{244}Pu	11.9 (1,0) ^{288}Fl	**9.91(1)**[g] **0.620** [d] -		**171** **0.328** **6**	$8 \cdot 10^{-7}$
07	237 36.5 ^{244}Pu	missing[h] (7,17) ^{288}Fl	9.92(1) - - -		**223** **0.0133** **13**	0.04
08	237 36.5 ^{244}Pu	13.6 (17,18) ^{288}Fl	**9.91(1)**[g] **2.408** - -	**9.33(1)** **0.0213**	**141+27** **0.000518** **10**	$3 \cdot 10^{-12}$
09	241 39.2 ^{244}Pu[a]	15.3 (23,18) ^{288}Fl	**9.93(1)**[b] **0.412** [d] -		**231** **0.00455** **2**	$8 \cdot 10^{-7}$
10	241 39.2 ^{244}Pu[a]	15.0 (22,11) ^{288}Fl	**9.92(1)**[b] **0.170** [d] -		**234+3** **0.165** **8**	$8 \cdot 10^{-7}$

TABLE I: Continued.

No.	$\langle E_{\rm lab}\rangle$ (MeV) $\langle E_{\rm com}\rangle$ (MeV) target[a]	$E_{\rm rec}$ (MeV) pixel (x,y) isotope	E_1 (MeV) Δt_1 (s) E_{ph} (keV) E_{e^-} (MeV)	E_2 (MeV) Δt_2 (s) E_{ph} (keV) E_{e^-} (MeV)	E_{SF} (MeV) Δt_{SF} (s) $N_{\rm Ge}$	$N_{\rm random}$
11	241 39.2 ^{244}Pu	14.6 (5,15) ^{288}Fl	**9.94(1)**[g] **0.748** - -		**241+16** **0.256** **6**	$8\cdot10^{-7}$
12	241 39.2 ^{244}Pu	14.6 (25,15) ^{288}Fl	**9.87(2)**[i] **0.0512** [d] -		**229** **0.456** **2**	$8\cdot10^{-7}$
13	241 39.2 ^{244}Pu	14.8 (12,15) ^{288}Fl	9.92(1) 0.860 - -		**172+18** **0.0280** **6**	$4\cdot10^{-4}$
14	241 39.2 ^{244}Pu	missing[h] (14,12) ^{288}Fl	**9.94(1)** - [d] -		**203** **0.00839** **6**	$9\cdot10^{-5}$

[a]For the first part of the experiment, the target wheel comprised one segment of enriched ^{242}Pu and three segments of enriched ^{244}Pu. For the second part of the experiment, all four segments of the target wheel were made of enriched ^{244}Pu.
[b]Event triggered 200-s beam shutoff.
[c]Event close to the beam-on period with many Ge crystals signaling.
[d]Delayed γ ray(s) observed within $\Delta t = [1, 7]$ µs. Delayed hits in the germanium detectors are disregarded in the interpretation because more than one randomly correlated hit of delayed character is expected [20].
[e]The random probability for a full-energy α-event in the energy interval [6,12] MeV being in prompt coincidence with an electron was < 0.01 for the experiment. See Ref. [20] for details.
[f]Escape event. See Ref. [20] for details.
[g]Event triggered 300-s beam shutoff.
[h]Implantation event searched for in a period of 8 s prior to the fission event concluding the decay chain.
[i]Reconstructed event; the detected energies were 0.56(1) MeV in the implantation detector and 8.86(1) MeV in the box DSSSD.

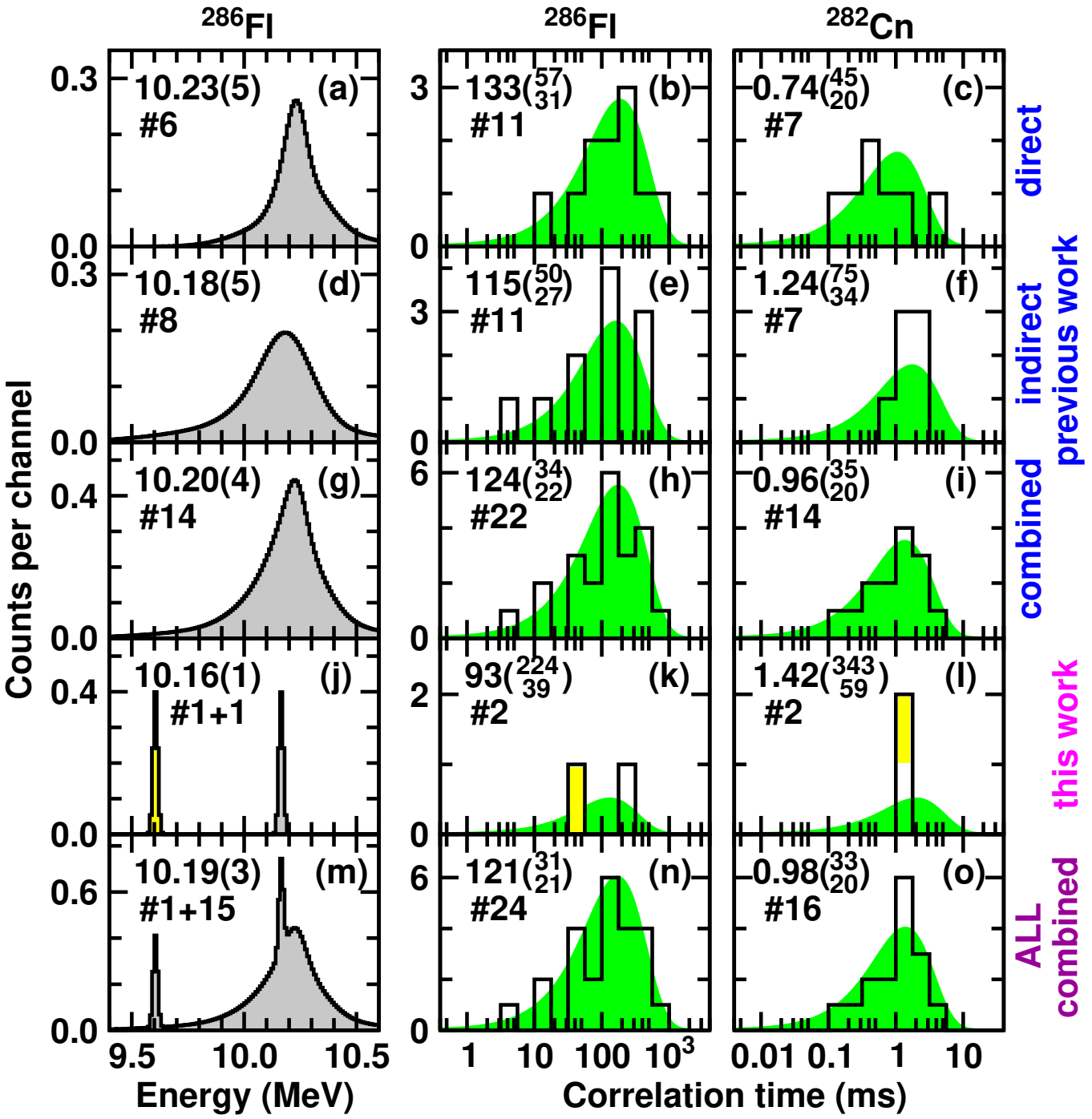

FIG. 1: (Color online) The left column provides experimental decay-energy spectra from events associated with the decay step $^{286}\mathrm{Fl} \rightarrow {}^{282}\mathrm{Cn}$. For a single entry, a Gaussian with integral one and a width compliant with its measured uncertainty was added into the respective spectrum. The numbers at the top left of each panel in the left column are the (α-decay) energies extracted by computing the histogram mean in the interval [9.9,10.5] MeV. The middle and right columns provide the correlation times for the decays of ^{286}Fl and ^{282}Cn, respectively. Experimental data points are comprised in the histograms (black lines). The shaded areas (green) provide correlation-time distributions expected for the corresponding half life, $T_{1/2}$, which are given in the top left corner of each panel. For all panels, the number behind the hashtag, #, indicates the number of available data points. The first row, panels (a)-(c), refers to previous direct production of ^{286}Fl [33–36]. The second row, panels (d)-(f), refers to previous indirect production of ^{286}Fl [37–39] The spectra in the third row, panels (g)-(i), are the sums of the spectra in the first and second row. The fourth row, panels (j)-(l), refer to the present data (cf. Table I). The event of main interest (excited state in ^{282}Cn, cf. chain 02 in Table I and main article) is highlighted with a yellow background. The spectra in the fifth row, panels (m)-(o), are the sums of the spectra in the third and fourth row, i.e. comprise current best values for the main decay characteristics of ^{286}Fl and ^{282}Cn.

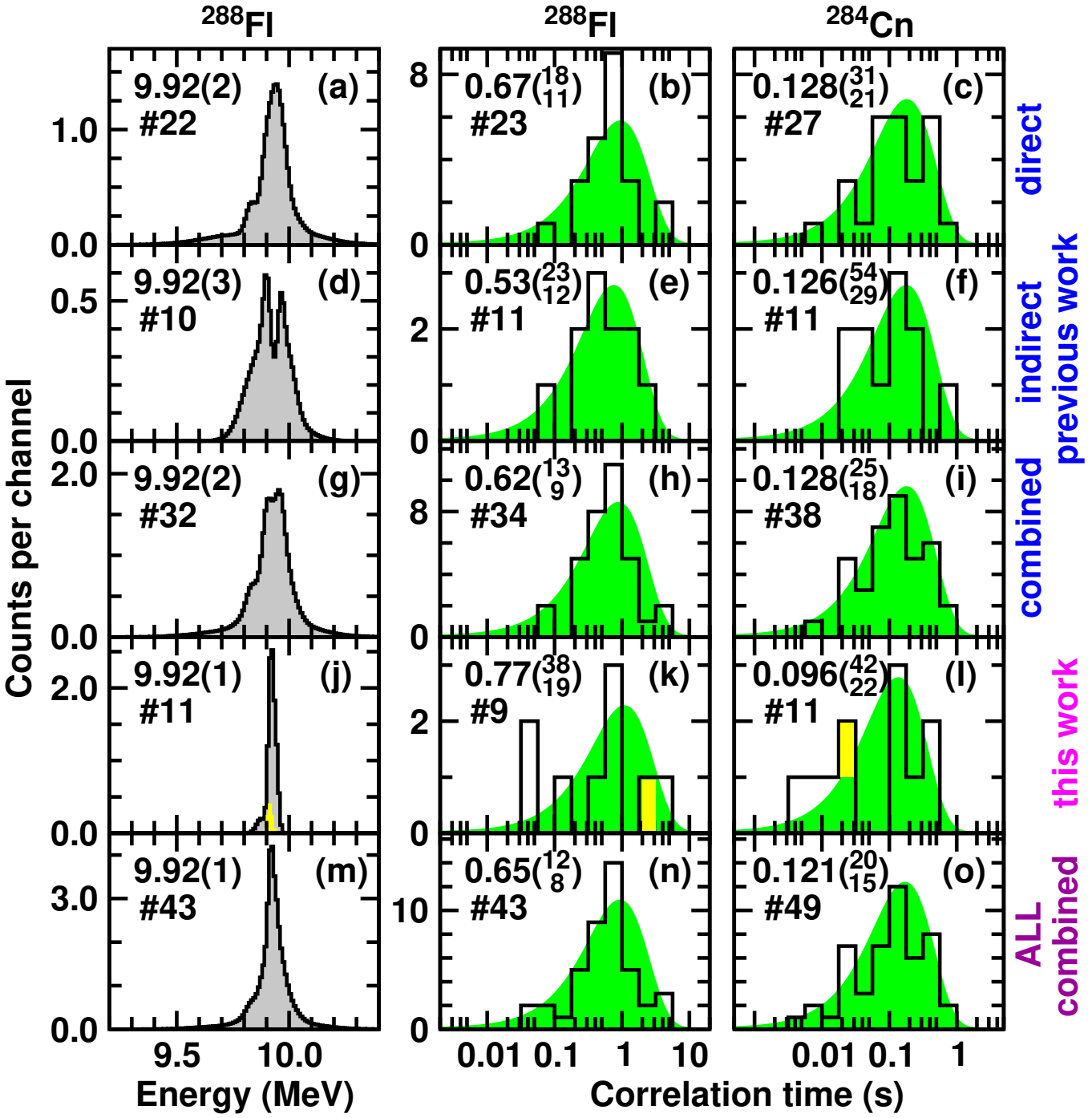

FIG. 2: (Color online) The left column provides experimental decay-energy spectra from events associated with the decay step ^{288}Fl$\rightarrow$ ^{284}Cn. For a single entry, a Gaussian with integral one and a width compliant with its measured uncertainty was added into the respective spectrum. The numbers at the top left of each panel in the left column are the (α-decay) energies extracted by computing the histogram mean in the interval [9.5,10.3] MeV. The middle and right columns provide the correlation times for the decays of ^{288}Fl and ^{284}Cn, respectively. Experimental data points are comprised in the histograms (black lines). The shaded areas (green) provide correlation-time distributions expected for the corresponding half life, $T_{1/2}$, which are given in the top left corner of each panel. For all panels, the number behind the hashtag, #, indicates the number of available data points. The first row, panels (a)-(c), refers to previous direct production of ^{288}Fl [4,8,9,28,33,37]. The second row, panels (d)-(f), refers to previous indirect production of ^{288}Fl [40–42]. The spectra in the third row, panels (g)-(i), are the sums of the spectra in the first and second row. The fourth row, panels (j)-(l), refer to the present data (cf. Table I). The event of main interest (discovery of ^{280}Ds, cf. chain 08 in Table I and main article) is highlighted with a yellow background. The spectra in the fifth row, panels (m)-(o), are the sums of the spectra in the third and fourth row, i.e. comprise current best values for the main decay characteristics of ^{288}Fl and ^{284}Cn.

TABLE II: Overview of correlation time analyses of single decay steps according to Ref. [43] of various ensembles of decay chains associated with previous direct ('Cn&Fl') and indirect ('Lv&Og') and present direct production of ^{286,288}Fl and ^{282,284}Cn, respectively. These are the same ensembles as displayed in the corresponding rows of Figs. 1 and 2.

Label	previous (Cn&Fl)	previous (Lv&Og)	previous	this work	all
^{286}Fl and ^{282}Cn					
No. of chains	11	16	27	2	29
References	[33–36]	[37–39]			
$T_{1/2}(^{286}\mathrm{Fl})$ (ms)	$133(^{57}_{31})$	$115(^{57}_{31})$	$124(^{34}_{22})$	$93(^{224}_{39})$	$121(^{31}_{20})$
data points; $\sigma_{\Theta_{\mathrm{exp}}}$	11 ; 1.00	11 ; 1.44	22 ; 1.26	2 ; 0.67	24 ; 1.22
$[\sigma_{\Theta,\mathrm{low}}, \sigma_{\Theta,\mathrm{high}}]$ [43]	[0.67,1.81]	[0.67,1.81]	[0.82,1.74]	[0.04,1.83]	[0.84,1.72]
data points; E_{decay} (MeV)	6 ; 10.23(5)[a]	8; 10.18(5)[a]	14; 10.20(4)[a]	1 ; 10.16(1)	15 ; 10.19(3)[a]
				1 ; 9.60(1)	1 ; 9.60(1)
$T_{1/2}(^{282}\mathrm{Cn})$ (ms)	$0.74(^{45}_{20})$	$1.24(^{75}_{34})$	$0.96(^{35}_{20})$	$1.42(^{343}_{59})$	$0.98(^{33}_{20})$
data points; $\sigma_{\Theta_{\mathrm{exp}}}$	7 ; 1.05	7 ; 0.43[b]	14 ; 0.92	2 ; 0.04	16 ; 0.87
$[\sigma_{\Theta,\mathrm{low}}, \sigma_{\Theta,\mathrm{high}}]$ [43]	[0.52,1.87]	[0.52,1.87]	[0.73,1.77]	[0.04,1.83]	[0.77,1.75]
^{288}Fl and ^{284}Cn					
No. of chains[c]	24	12	36	11	47
References	[4,8,9,28,33,37]	[40–42]			
$T_{1/2}(^{288}\mathrm{Fl})$ (s)	$0.67(^{18}_{11})$	$0.53(^{23}_{12})$	$0.62(^{13}_{9})$	$0.77(^{38}_{19})$	$0.65(^{12}_{8})$
data points; $\sigma_{\Theta_{\mathrm{exp}}}$	23 ; 0.87	11 ; 0.91	34 ; 0.88[b]	9 ; 1.48	43 ; 1.04
$[\sigma_{\Theta,\mathrm{low}}, \sigma_{\Theta,\mathrm{high}}]$ [43]	[0.83,1.73]	[0.67,1.81]	[0.91,1.65]	[0.62,1.84]	[0.95,1.61]
data points; E_{decay} (MeV)	22 ; 9.92(2)[d]	10; 9.92(3)[d]	32; 9.92(2)[d]	11 ; 9.92(1)[d]	43 ; 9.92(1)[d]
$T_{1/2}(^{284}\mathrm{Cn})$ (ms)	$128(^{31}_{21})$	$126(^{54}_{29})$	$128(^{25}_{18})$	$96(^{42}_{22})$	$121(^{20}_{15})$
data points; $\sigma_{\Theta_{\mathrm{exp}}}$	27 ; 1.05	11 ; 1.03	38 ; 1.05	11 ; 1.52	49 ; 1.20
$[\sigma_{\Theta,\mathrm{low}}, \sigma_{\Theta,\mathrm{high}}]$ [43]	[0.87,1.69]	[0.67,1.81]	[0.93,1.63]	[0.67,1.81]	[0.97,1.59]

[a]Result from the integration of the energy spectra in the left column of Fig. 1 in the interval [9.9,10.5] MeV.
[b]The experimental value for $\sigma_{\Theta_{\mathrm{exp}}}$ falls outside the confidence limit, but such that the agreement with a single decay curve rather fits too well. See Fig. 1(f).
[c]Half-life analysis of ^{284}Cn includes in addition four decay chains from element 114 chemistry experiments behind TASCA [8,9].
[d]Result from the integration of the energy spectra in the left column of Fig. 2 in the interval [9.5,10.3] MeV.